

Characteristics of ocean waters reaching Greenland's glaciers

Fiammetta STRANEO,¹ David A. SUTHERLAND,² David HOLLAND,³ Carl GLADISH,³
Gordon S. HAMILTON,⁴ Helen L. JOHNSON,⁵ Eric RIGNOT,^{6,7} Yun XU,⁶
Michele KOPPES⁸

¹*Department of Physical Oceanography, Woods Hole Oceanographic Institution (WHOI), Woods Hole, MA, USA*
E-mail: fstraneo@whoi.edu

²*Department of Geological Sciences, University of Oregon, Eugene, OR, USA*

³*Center for Atmosphere–Ocean Science, New York University, New York, NY, USA*

⁴*Climate Change Institute, University of Maine, Orono, ME, USA*

⁵*Department of Earth Sciences, University of Oxford, Oxford, UK*

⁶*Department of Earth System Science, University of California, Irvine, Irvine, CA, USA*

⁷*Jet Propulsion Laboratory, California Institute of Technology, Pasadena, CA, USA*

⁸*Department of Geography, University of British Columbia, Vancouver, Canada*

ABSTRACT. Interaction of Greenland's marine-terminating glaciers with the ocean has emerged as a key term in the ice-sheet mass balance and a plausible trigger for their recent acceleration. Our knowledge of the dynamics, however, is limited by scarcity of ocean measurements at the glacier/ocean boundary. Here data collected near six marine-terminating glaciers (79 North, Kangerdlugssuaq, Helheim and Petermann glaciers, Jakobshavn Isbræ, and the combined Sermeq Kujatdleq and Akangnardleq) are compared to investigate the water masses and the circulation at the ice/ocean boundary. Polar Water, of Arctic origin, and Atlantic Water, from the subtropical North Atlantic, are found near all the glaciers. Property analysis indicates melting by Atlantic Water (AW; found at the grounding line depth near all the glaciers) and the influence of subglacial discharge at depth in summer. AW temperatures near the glaciers range from 4.5°C in the southeast, to 0.16°C in northwest Greenland, consistent with the distance from the subtropical North Atlantic and cooling across the continental shelf. A review of its offshore variability suggests that AW temperature changes in the fjords will be largest in southern and smallest in northwest Greenland, consistent with the regional distribution of the recent glacier acceleration.

INTRODUCTION

Net mass loss from the Greenland ice sheet more than doubled over the last decade due, to a large extent, to increased ice discharge from the acceleration and retreat of outlet glaciers from the western and southeastern sectors (Rignot and Kanagaratnam, 2006; Van den Broeke and others, 2009). This 'dynamic thinning' is a highly nonlinear and poorly understood process; it is absent from climate models and considered the largest source of uncertainty for sea-level rise predictions for the 21st century (Solomon and others, 2007). Both ice-flow models (Nick and others, 2009; Vieli and Nick, 2011) and high-resolution laser altimetry (Pritchard and others, 2009) indicate that the acceleration began at the tidewater termini of the outlet glaciers, in Greenland's deep, long fjords. One leading hypothesis is that it resulted from increased submarine melt rate at the termini, leading to the thinning and ungrounding of the ice tongue, and a reduction in frontal buttressing to glacier flow (Thomas, 2004; Holland and others, 2008; Motyka and others, 2011). This hypothesis is supported by observations of warming ocean waters on Greenland's western shelf (Holland and others, 2008; Motyka and others, 2011), due to the accumulation of Atlantic Water (of subtropical origin) in the Subpolar Gyre (Bersch and others, 2007; Thierry and others, 2008). It is also consistent with recent paleo-reconstructions linking glacier activity to changes in the ocean properties on the continental shelves (Lloyd and others 2011; Andresen and others 2012). The implication is that ocean variability around Greenland may have a sizable impact on the ice-sheet mass balance. Thus, glacier/ocean interactions must be accounted

for in order to understand (and predict) changes in Greenland's marine-terminating glaciers.

Growing interest in the oceanic forcing of the glaciers has led to increasing surveys of Greenland's glacial fjords (Holland and others 2008; Rignot and others 2010; Straneo and others 2010; Christoffersen and others 2011; Johnson and others 2011) which, until recently, were largely unexplored. For those fjords associated with Greenland's large glaciers, however, these surveys typically fail to cover the region near the grounding line. For the quasi-vertical large tidewater glaciers in southwestern and southeastern Greenland (e.g. Helheim and Kangerdlugssuaq Glaciers and Jakobshavn Isbræ), the 'no-data' region extends 5–10 km from the terminus due to the vigorous calving and the presence of an ice melange. For glaciers in North Greenland, the presence of ice tongues which extend several tens of kilometers implies that, without drilling through ice that is hundreds of meters thick, these surveys typically end at the edge of the tongue. Thus, without exception, these surveys have failed to sample the ice/ocean boundary layer where the meltwater-laden plume is expected to rise (Jenkins, 2011). Without measurements from this boundary layer, there is no a priori way to deduce which water masses actually reach and melt the glaciers from the 'far field' measurements. This problem could be circumvented if one knew the circulation that transports unmodified waters towards the glacier and glacially modified waters away from it. Velocity measurements from the fjords (e.g. Rignot and others 2010; Straneo and others 2010, 2011; Mortensen and others 2011; Sutherland and Straneo, 2012), however,

have revealed the fjord circulation to be complex and highly variable, suggesting that the 'melt' circulation may not be a simple estuarine cell as observed by Motyka and others (2003) for Columbia Glacier, Alaska.

Insight into the dynamics at the glacier/ocean boundary, however, can be gained by investigating the transformation of ocean waters by the glacier in conjunction with thermodynamic theories for ice melting in saline waters (Gade, 1979; Jenkins, 1999). This approach was recently applied to data collected near Helheim Glacier, southeast Greenland, (Straneo and others, 2011) to show that summer melting is potentially driven by the Polar (PW) and Atlantic Water (AW) present in the fjord and is influenced by significant subglacial discharge at depth. (By contrast in winter, the PW is too cold to drive melting and there is no evidence of subglacial discharge.) A comparable approach was applied to summer surveys from Petermann Fjord (Johnson and others, 2011).

Here oceanographic data collected from the vicinity of five major marine-terminating glaciers (glaciers, hereafter) distributed around Greenland are analyzed and compared using this method. Additional data from a fjord where two smaller glaciers drain are included for comparison. The overarching goal is to compare properties of the water masses near the glaciers and, where possible, to identify those that have been modified by the glacier. A second goal is to identify common characteristics that can provide insight into the dynamics at the ice/ocean boundary. Lastly, these findings are discussed in the context of the large-scale ocean circulation around Greenland. While the analysis presented is mostly restricted to a single survey for each fjord, context for the general validity of these results is discussed where more data are available. Since there is no simple relation between water properties and submarine melt rates, we do not provide estimates of the latter. Still, we believe that the analysis presented is a first step towards understanding the oceanic controls on submarine melting of glaciers around Greenland.

DATA

We use temperature and salinity profiles collected in the vicinity of five major glaciers which, clockwise from the northeast (Fig. 1), are: Nioghalvfjerdsbræ (or '79 North Glacier'; 79NG), Kangerdlugssuaq Gletscher (KG), Helheim Gletscher (HG), Jakobshavn Isbræ (JI) and Petermann Gletscher (PG). Data from Torsukatak Fjord (TF), where the smaller Sermeq Avangnardleq and Kujatdleq drain, are included to provide a comparison with a medium-sized system. The glacier/fjord system is referred to using the acronym in parenthesis. Profile locations and data are shown in Figure 2. Data for the first three (79NG, KG and HG) consist of conductivity–temperature–depth (CTD) profiles collected in August and early September 2009 from an icebreaker. They were collected using a 6 Hz XR-620 RBR CTD, and water samples were collected at a range of depths and on multiple casts to calibrate salinity. One additional profile from HG, collected in March 2010 using expendable CTDs (XCTDs) launched from a helicopter and cross-calibrated with a CTD in the upper 50 m, is included for a comparison of the 'winter' conditions. The HG data are described by Straneo and others (2011). At 79NG, two additional CTD profiles were collected through a rift in the floating ice tongue (Fig. 2) accessed by helicopter. Data for JI

were collected in late July/early August 2009 using XCTDs deployed from a helicopter. Cross-calibration of the XCTDs was achieved by comparing XCTD and CTD profiles (taken using a Seabird SBE 19plus CTD) collected at the fjord mouth from a small local vessel. Data from Torsukatak Fjord (TF) were collected using a Seabird SBE 19 CTD from a small boat in August 2010. For PG we use data collected in summer 2003 and described by Johnson and others (2011), together with a profile collected in May 2004 by drilling through the floating ice tongue (Rignot and Steffen, 2008).

METHODS

The analysis presented relies on identifying within each survey a 'near' and a 'far' set of profiles: the *glacier* and *ambient* profiles, respectively. Ideally the latter reflect ambient waters close enough to potentially come in contact with the ice but far enough away that they do not contain glacially modified waters. The *glacier* profiles are those closest to the grounding line (where the bulk of the melting is thought to occur (e.g. Jenkins, 2011)) and contain waters that have interacted with the glacier. Under the assumptions that conditions vary slowly compared to the duration of the survey (typically 1 or 2 days), that the along-fjord variability is much larger than the across-fjord variability (confirmed where data are available and discussed by Straneo and others, 2011) and that the modification of properties from the ambient to the glacier profiles is due to interaction with the glacier alone (Straneo and others 2011), a comparison of the profiles will provide information on the glacier-induced transformation of the ambient waters. Of the glaciers sampled, 79NG and PG have floating ice tongues 70–80 km long and hundreds of meters thick (Mayer and others, 2000; Rignot and Steffen, 2008). At 79NG the glacier profiles, collected in the rift of the ice tongue, are representative of the region where the tongue is ~100 m thick (Fig. 2). For the ambient profiles we use profiles collected on the shelf, where a recirculation around Belgica Bank provides the source waters that flow under the glacier (Budéus and others, 1997). At PG the 2003 survey extended to the front of the floating ice tongue (Fig. 2) ~70 km from the grounding line, and this profile is used as the glacier profile. As ambient profiles, we choose those collected north of the fjord's mouth, in Nares Strait, since the flow in the strait, feeding the waters under PG's tongue, is from north to south (Münchow and others, 2011). For PG a single profile collected through the ice tongue in May 2004 is taken to represent glacier conditions in winter (Rignot and Steffen, 2008; Johnson and others, 2011). The remaining glaciers have no known sizable ice tongue and are thought of as mostly vertical faces. For these systems, the glacier profiles are those collected closest to the glacier's edge and the ambient profiles are those from sections across or near the mouth of the fjords.

The location of the glacier and ambient profiles for each system are shown in Figure 2, together with the potential temperature (temperature, hereafter), practical salinity (salinity, hereafter) and stratification (Brunt-Väisälä frequency squared) profiles with depth and temperature versus salinity (*T/S*, hereafter) diagram. The profiles collected between the ambient and glacier profiles (where they exist) show a progressive transition from one to the other (not shown). Two lines are overlaid on the *T/S* diagram: a melting and a runoff line. The melting line is where the properties of a mixture of

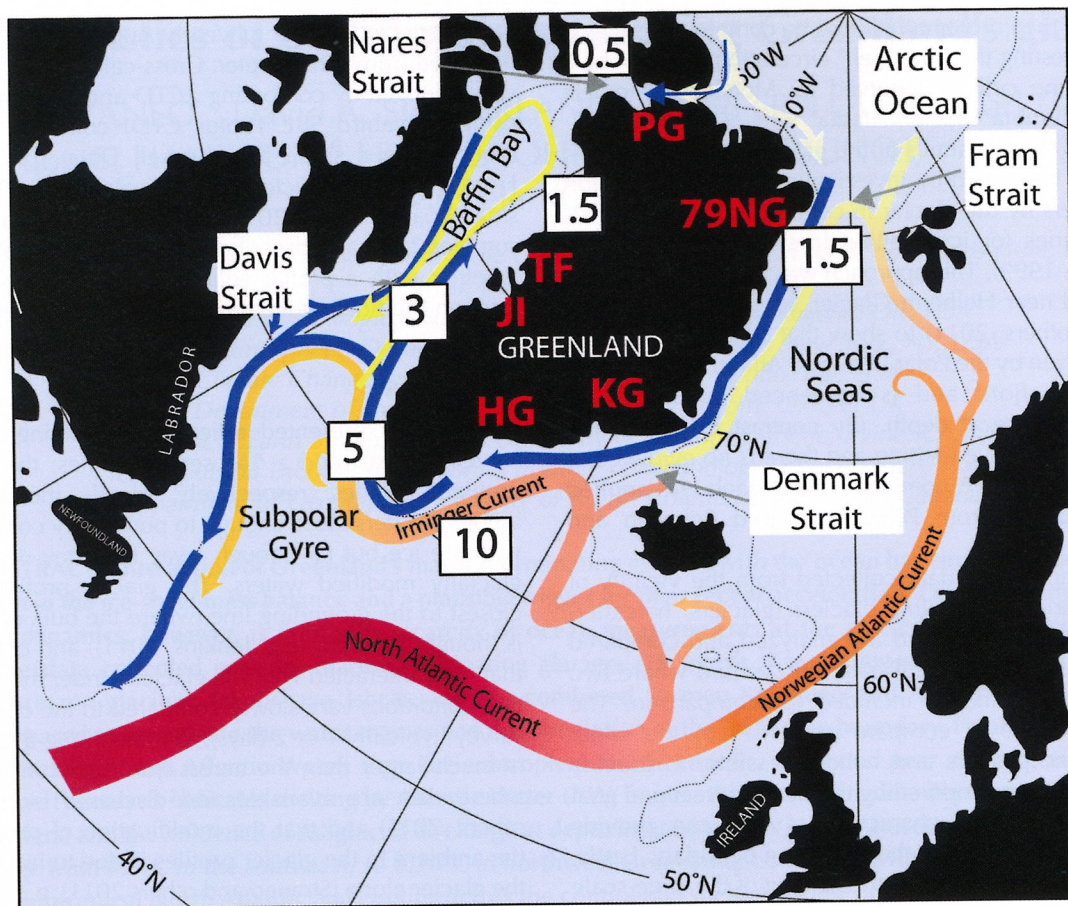


Fig. 1. Schematic circulation of Atlantic Water (red to yellow) and Polar Water (blue) in the northern North Atlantic (Subpolar Gyre), the Nordic Seas and part of the Arctic Ocean. Numbers indicate the mean temperature of the AW circulating offshore. The locations of the six glacial fjords are shown in red. The circulation is revised from McCartney and Talley (1984), using the review by Schott and Brandt (2007) and observations (Fratantoni, 2001; Bower and others, 2002; Orvik and Niiler, 2002; Jakobsen and others, 2003) for the Subpolar Gyre. The Nordic Seas circulation is updated using Hansen and Østerhus (2000), Orvik and Niiler (2002) and Jakobsen and others (2003); and Schauer and others (2008) and de Steur and others (2009) for Fram Strait. The flow of AW around the Labrador Sea and into Baffin Bay is described by Cuny and others (2005) and Münchow and others (2006). The source waters for Nares Strait are described by Münchow and others (2011).

ambient water and meltwater would fall and is indicative of waters transformed by submarine melting of glacial ice. It is estimated according to Jenkins (1999) in which θ_{eff} (the 'effective ice temperature'), which takes into account the amount of energy required to melt ice, is

$$\theta_{\text{eff}} = \theta_f - \frac{L}{C_p} - \frac{C_i}{C_p}(\theta_f - \theta_i)$$

where θ_f is the freezing-point temperature of water with salinity equal to that in the glacier profiles at the grounding line depth, L is the latent heat of fusion for ice ($334\,500\,\text{J kg}^{-1}$), θ_i is the actual ice temperature (taken to be -15°C), and C_i and C_p are the specific heat capacities of ice and water respectively (2100 and $3980\,\text{J kg}^{-1}\text{K}^{-1}$). We stress that the melting-line slope is not very sensitive to the values of the ice or freezing-point temperature chosen (see also Jenkins, 1999). As a starting point for the melting line, we use the T/S characteristics of the densest (typically the warmest) waters in the glacier profiles. The runoff line is where a mixture of ambient/meltwater and runoff (defined as water with zero temperature and salinity) would fall in T/S space. As a starting point of the runoff line we choose the deepest point in T/S space where the curves deviate significantly from the melting line. We label this point the RP ('runoff point') for reasons explained below. The ice flux, the

grounding line and sill depth (where known) and the distance of the glacier profiles from the grounding line for the glaciers are listed in Table 1. For TF, we cannot distinguish the contribution from either glacier (Fig. 2); hence we report values for both.

RESULTS

The ambient profiles contain a thick layer (several hundred meters) of warm, salty water below a cold, fresh layer, with stratification rapidly increasing at the interface of the two. The properties and T/S characteristics of these two water types are consistent with modified AW and PW flowing around Greenland's shelf (see below). At the surface, the waters in the ambient profiles are typically fresher and warmer, consistent with terrestrial runoff, or surface ice melt, and summer surface heating. By contrast, the surface water near the glaciers is colder and fresher. (The glacier profiles at PG and 79NG did not sample surface waters because of the ice tongue.) A comparison of the glacier and ambient profiles shows that the properties are usually similar at depth. JI is an exception, since the deep waters in the glacier profiles are considerably fresher and colder than those in the ambient profiles. We attribute this to JI's relatively shallow ($\sim 250\,\text{m}$; Table 1) that isolates the deeper fjord waters. At

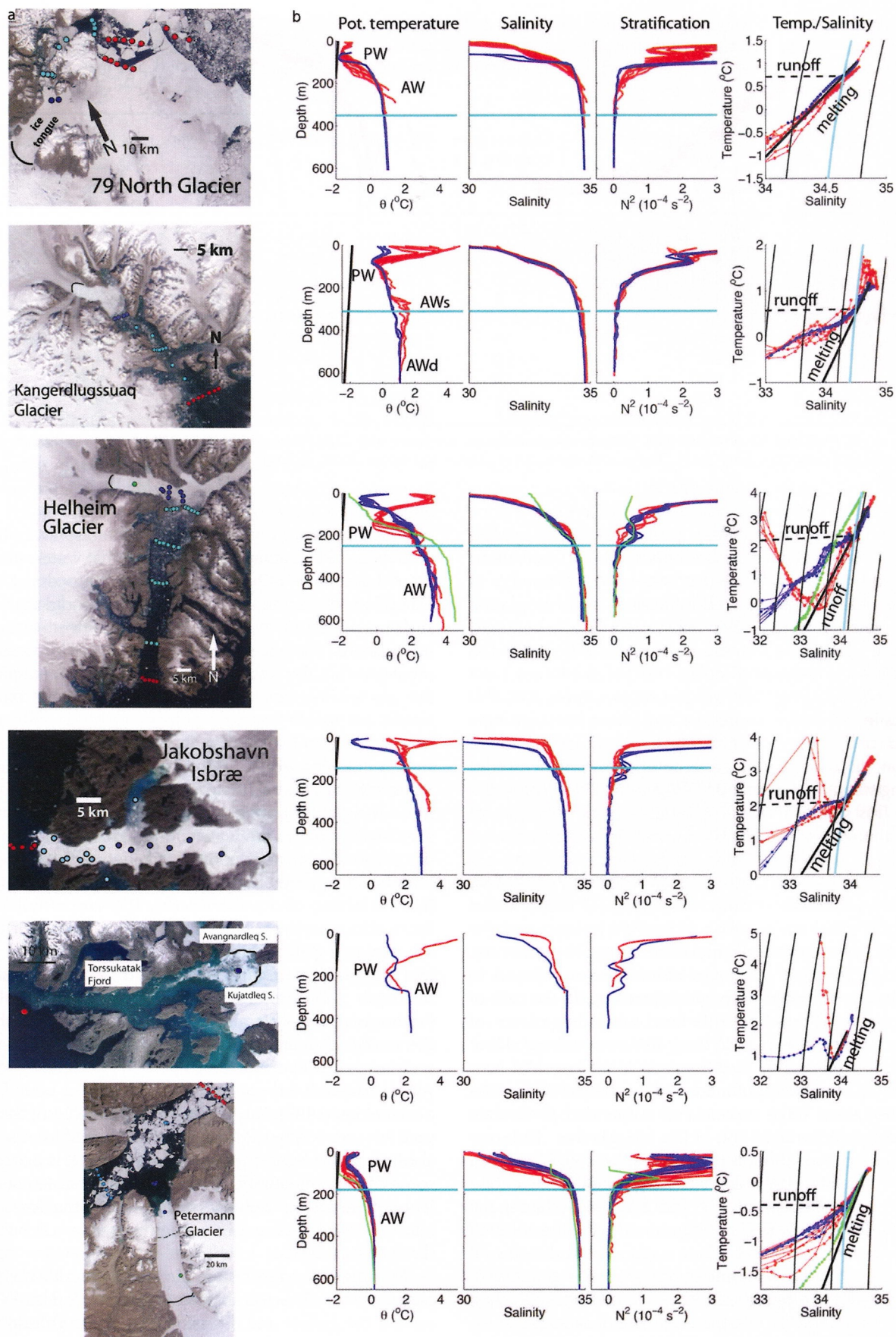


Fig. 2. (a) Satellite images of the six glaciers and glacial fjords with the station location (red is for the ambient profiles, blue for the glacier profiles, cyan for other profiles collected in the same survey). Winter glacier profiles from HG and PG are shown in green. (b) (Left to right): potential temperature, salinity, stratification as a function of depth and T/S plot for all the glacier and ambient profiles (where available). The glaciers/glacial fjords are shown in order from the northeast to the northwest corner (79NG, KG, HG, JI, TF, PG). The melting (solid black thick) and runoff (dashed black thick) lines are overlaid on all the T/S plots, along with fixed isopycnals (solid thin black). The cyan line indicates the depth of the RP (see text) in the depth profiles and its density in the T/S plots.

Table 1. Glacier and water characteristics for the systems studied, listed in order of decreasing AW temperature (see text for glacier/system full name). The AW (potential) temperature and salinity listed are those found at the grounding line depth in the glacier profiles (Fig. 2). The RP properties are shown in Figure 2 by cyan lines. For HG and PG, (w) indicates the winter survey data. Sill depths indicated are for sills at the mouth of the fjord

Glacier	Mean ice flux ¹	Grounding depth	Sill depth	Distance from grounding line	AW temp.	AW salinity	RP temp.	RP sal.	RP depth
	Gta ⁻¹	m	m	km	°C		°C		m
HG	32	600–700 ²	600 ³	10	3.46	34.70	2.42	34.35	250
HG (w)	32	600–700	600	5	4.5	34.76	–	–	–
JI	35	800 ²	255 ⁴	20	2.97	34.25	2.23	33.93	150
TF Av.	2.7	450 ⁵	285 ⁶	5	1.8	34.16	–	–	–
TF Kuj.	5.7	450 ⁵	285	7	1.8	34.16	–	–	–
KG	37	600–700 ²	650 ³	10	1.17	34.75	0.61	34.50	310
79NG	15	600 ⁷	700 ⁷	60	1.0	34.75	0.72	34.65	350
PG	12.8	600 ⁸	350 ⁸	70	0.16	34.75	−0.40	34.41	160
PG (w)	12.8	600	350	15	0.16	34.75	−1.09	34.19	150

¹E. Rignot and others (unpublished information). ²<https://www.cresis.ku.edu/data/greenland>. ³Schjøth and others (2012). ⁴Schumann and others (in press).

⁵E. Rignot (personal communication, 2012). ⁶Rignot and others (2010). ⁷Mayer and others (2000). ⁸Johnson and others (2011).

TF, the uniformity of the deep properties in the glacier profiles is also indicative of a ~285 m sill. In the systems considered here, the sills are deep enough to allow AW to reach the vicinity of the glaciers (at least as far as the glacier profiles were collected). For fjords with shallower sills, however, it is likely that the inflow of AW may be limited as found by Mortensen and others (2011) for Nuuk and Kangia Nunata, where the sill is ~80 m. Unlike AW, PW observed in the ambient profiles has either been strongly modified or is absent in the glacier profiles (KG is an exception, discussed below). In general, the ambient profiles are strongly stratified from the PW/AW interface towards the surface. This stratification is mostly preserved in the glacier profiles, though with some differences (discussed below).

In the T/S diagrams, the deep glacier and ambient characteristics are similar and overlap with the melting line. This could either be because the ambient PW/AW curve coincides with the melting line or it could indicate that the deep waters contain glacially modified waters. In either case, this means that the T/S curves alone cannot be used to identify waters transformed by glacial melting. In the case of HG, Straneo and others (2011) used two other pieces of evidence to conclude that the deep AW was melting HG at the grounding line depth. First the deep AW was colder near the glacier than at the mouth. Second the deep AW near the glacier contained large amounts of suspended particulate which suggested interaction with the glacier. Turbidity profiles are not available for the surveys discussed here, but in all cases the deep AW (near or at the grounding line depth) in the glacier profiles is slightly colder and fresher than in the ambient profiles. This finding, combined with the inferred plume dynamics discussed below, supports the conclusion that the deep AW are reaching and melting the glaciers. In Table 1, we list the properties of the AW at the grounding line depth. These should be interpreted as the densest (typically warmest) AW likely reaching and melting the glaciers, with the caveat that direct evidence of this can only come from measurements at the glacier/ocean boundary.

Above the layer where the ambient, glacier and melting T/S lines overlap, there exists a 'runoff' point (RP), in most systems, above which the T/S characteristics of the glacier profiles veer from the melting line towards the runoff line

(Fig. 2). For most systems, the veering is also away from the ambient T/S characteristics, implying that waters above this point have been transformed by some process. KG is an exception discussed below. Possible candidates include surface processes (e.g. wind mixing, heat loss to the atmosphere, sea/ice interaction) or internal processes (e.g. mixing within the water column) as well as interaction with the glacier. We rule the first out on the basis that these waters are well below the reach of a mixed layer (especially in summer) and also that the water column is strongly stratified (which would limit the reach of surface processes). As for internal mixing, the properties of the waters above the RP in the glacier profiles cannot be explained by mixing of the deeper waters with waters found closer to the surface in the ambient profiles. Support for the notion that these waters have been modified by interaction with the glacier is found by noting that, above the RP, the T/S curves fall between the melting and runoff lines, consistent with a transformation by two glacier-driven mechanisms: submarine melting and discharge of runoff (either due to surface or basal melt) at depth (here referred to as 'subglacial discharge'). Furthermore the waters located just above the depth of the RP in the glacier profiles are warmer than the ambient profiles, consistent with the upwelling of glacier-modified AW (freshened and cooled) at the ice/ocean boundary (see also Jenkins, 1999). Farther up the water column, the glacier profiles are colder than the ambient profiles, indicating cooling due to interaction with the glacier. It is possible that some of the ambient water transformation is also due to the icebergs found in the ice melange. But the ice melange alone would not explain the presence of subglacial discharge at depth.

To explain the distribution of glacially modified water, we propose the following interpretation. At depth, AW flows toward the glacier and drives melting at the grounding line, resulting in upwelling at the ice/ocean boundary. The upwelling plume(s) is also enhanced by subglacial discharge at the grounding line (Jenkins, 2011) or above it. Much of this subglacial discharge is likely to occur through a limited number of drainage channels and to be highly seasonal (e.g. Mernild and Basholt, 2009; Andersen and others, 2010). This means that, even at its peak in summer, one expects

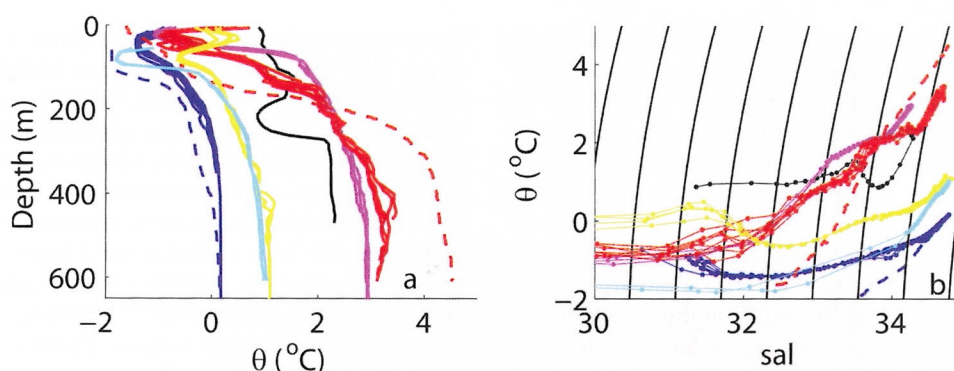


Fig. 3. (a) Potential temperature and (b) potential temperature/salinity for the glacier profiles of all the systems. Dashed lines represent the winter surveys. Isopycnal surfaces are overlaid (black thin lines).

strong spatial variations in the upwelling, with highly buoyant, localized plumes initiated by subglacial discharge and a more distributed, less buoyant upwelling due to submarine melting alone. This likely gives rise to a range of plumes rising and entraining 'ambient' water in a stratified environment. Whether these plumes rise to the surface or reach their level of neutral buoyancy at depth depends on their initial buoyancy anomaly, on the accumulation of meltwater and on the stratification of the nearby waters (Huppert and Josberger, 1980; Huppert and Turner, 1980). This is a complex and coupled problem since the stratification of waters at the ice/ocean boundary, in turn, is strongly controlled by the boundary layer processes. For example, the glacially modified waters found just above the RP are often associated with a localized stratification maximum (e.g. HG in summer and winter and PG in winter).

Under the assumption that a plume's evolution is, to first order, due to buoyant fluid rising in the stratified environment, one would expect plumes with a small buoyancy anomaly, i.e. those which do not contain much subglacial discharge, to equilibrate rapidly (within a few tens/hundreds of meters of the grounding line) while plumes characterized by a large buoyancy anomaly (e.g. those fed by a drainage channel) would rise higher up the water column and potentially reach the surface. These scenarios are supported by the recent analytical and numerical modeling of Jenkins (2011) and Xu and others (2012) for plumes rising at the edge of fairly steep glacier faces (at least near the grounding line). For glaciers where the slope of the ice/ocean boundary is much more horizontal, other sources of turbulence may dominate. In either case, once the waters carried within a plume reach their neutrally buoyant depth they will flow away from the glacier along density surfaces which (outside of the plume) are mostly horizontal. Profiles collected near the glaciers (but outside of the turbulent plume region) will therefore cut across multiple export pathways of glacially modified waters and the associated inflow pathways of unmodified water. At depth, where any glacially modified waters must have rapidly equilibrated, we expect to find waters modified by the addition of meltwater alone, consistent with the finding that the T/S characteristics of the deep waters near the glaciers fall on the melting line. Higher up the water column, we expect to find glacially modified waters from plumes fed by glacial melt and subglacial discharge, consistent with the observation that, above the RP, the T/S characteristics reflect the combined effects of melting and runoff.

Among the systems sampled, JI, HG and KG show the most pronounced veering towards the runoff line above the RP, consistent with their relatively southern latitude and the summer occupation of the surveys (Figs 2 and 3). 79NG shows minimal influence of subglacial discharge. This could be because this survey was taken in early September when all of the surface melt ponds had either drained or refrozen. At PG, the partial overlap of the ambient and glacier profiles in the upper layers makes it difficult to distinguish ambient or modified waters. This is likely because the 'glacier' profile at PG in the 2003 survey is ~70 km from the grounding line. At KG the problem appears to be the opposite. It looks like the mouth waters contain large volumes of glacially modified waters in the upper layer while there is little signature of the PW. At TF, the limited number of profiles makes it difficult to build a coherent picture. Nonetheless, the deep waters fall along the melting line, and closer to the surface the T/S properties in the glacier profile are indicative of freshening by runoff/subglacial discharge. Finally, the two available 'winter' profiles, collected in May at PG and in March at HG, support the interpretation proposed above since, at the time when these winter surveys were occupied, subglacial discharge is at a minimum. Indeed, their T/S characteristics are mostly along the melting line and there is little or no sign of runoff discharge at depth (green lines in Fig. 2).

The analysis presented here is confined to a single survey for each fjord (or two at the most). Yet the results obtained, including the shape of the T/S curves, the layering of PW and AW, and the AW properties, are largely confirmed by other summer surveys conducted in these fjords. These include the surveys conducted in 2007 and 2009 at PG (Johnson and others, 2011), in 2008 at JI (Holland and others, 2008), in 2008 at HG (Straneo and others, 2010) as well as in 2010 and 2011 (not shown), in 1993 and 2004 at KG (Azetsu-Scott and Tan, 1997; Christoffersen and others, 2011) and in 1997 near 79NG (Mayer and others, 2000). The fact that these general characteristics hold for multiple glacier/fjord systems and for multiple surveys suggests that they are indicative of the dominant mechanisms occurring at the glacier/ocean interface.

ORIGIN OF THE ATLANTIC WATER FOUND IN THE FJORDS

Our results indicate that the warmest (deep) AW is found near HG, JI and TF followed by KG and 79NG, with PG having the coldest (Table 1; Fig. 3a and b). This grouping is

consistent with the distinct pathways taken by AW to reach the three ocean basins at Greenland's margins: the Subpolar Gyre, the Nordic Seas and the Arctic Ocean (Fig. 1). AW in the Subpolar Gyre, carried by the Irminger Current along Greenland's southeastern and western continental margins, is the warmest because of its proximity to the source. These waters cool as they flow around the Subpolar Gyre (due to surface heat loss and mixing with the PW) from a mean temperature of the AW core of $\sim 10^{\circ}\text{C}$ in southeast Greenland (Väge and others, 2011), to $5\text{--}7^{\circ}\text{C}$ in the Labrador Sea (Pickart and Spall, 2007), 3°C in Davis Strait (Curry and others, 2011) and 1.5°C in Baffin Bay (Zweng and Münchow, 2006) (Fig. 1). This branch retroflects south of Nares Strait because of a sill (e.g. Münchow and others, 2011). A second branch of AW flows into the Nordic Seas and is also progressively cooled such that, by the time it reaches Fram Strait, it has temperatures of $2\text{--}3^{\circ}\text{C}$ (Isachsen and others, 2007). Here some of the AW recirculates to the south (also known as return Atlantic Water (RAW; e.g. Schauer and others, 2008)), feeding the branch of AW found along the continental shelf of northeast Greenland, whose temperatures are $\sim 1\text{--}2^{\circ}\text{C}$ (Schauer and others, 2008). From there on, AW is found beneath PW flowing out the Arctic and thus mostly preserves its heat content as it is isolated from the atmosphere. These waters can be tracked all the way to Denmark Strait (e.g. Isachsen and others, 2007; Fig. 1). Finally, the Arctic branch is fed by AW that has transited the Nordic Seas and continued towards the Arctic Ocean, where it circulates cyclonically around the entire basin, explaining the cold $\sim 0.1^{\circ}\text{C}$ modified AW found in Nares Strait, near PG (Münchow and others, 2011).

The AW temperatures at the edge of the continental shelf, where the core of the current is located, are in all cases warmer (and saltier; not shown) than those observed in the nearby fjords. This is likely due both to surface cooling (where the AW is close to or at the surface) and to mixing with the cold, fresh PW carried by the East and West Greenland Currents (Cuny and others, 2005; Sutherland and Pickart, 2008). The largest cooling occurs for HG where the shelf is widest. Even if cooler, the deep AW in the fjords still reflects the AW properties in the different ocean basins (Fig. 3). The AW found at HG, JI and TF is fed by the Subpolar Gyre pathway and is the warmest, the AW found at 79NG is fed by the Nordic Seas pathway and is colder, while the water at PG is fed by the Arctic pathway and is the coldest (Johnson and others, 2011; Münchow and others, 2011). KG is more complex since it is located at Denmark Strait, and appears to contain AW fed both by the Nordic Seas and the Subpolar Gyre pathways. This can be inferred by considering that the deep AW in Kangerdlugssuaq Fjord (AWd in Fig. 2) is identical (in T/S space) to that found at 79NG, while higher up the water column the subsurface temperature maximum tends towards the Subpolar Gyre AW properties (AWs in Fig. 2; see also profiles shown in Christoffersen and others, 2011). This shallower AW is consistent with AW that flows into the fjord via Kangerdlugssuaq Trough (Sutherland and Pickart, 2008). Unlike the deep AW, the shallower AW is not evident in the glacier profiles, suggesting it has been transformed by mixing (potentially with glacially modified waters).

One of the leading hypotheses to explain the recent acceleration of Greenland glaciers is that a warming of ocean waters coming in contact with the glaciers resulted in a change at the ocean/ice boundary which, in turn, triggered

the glaciers' acceleration (e.g. Holland and others, 2008). Given this, it is important to know how large a change in AW temperature one expects to see in the fjords. While there are not enough fjord measurements to establish this directly, a likely magnitude for the range can be inferred from measurements on the continental shelf in the vicinity of the fjord. Historical data show that these are largest in the Subpolar Gyre, where interannual changes of $1\text{--}2^{\circ}\text{C}$ are not uncommon over the past 50–60 years (Holland and others 2008; Motyka and others 2011; Andresen and others 2012), followed by Baffin Bay where changes of $0.5\text{--}0.8^{\circ}\text{C}$ are observed in the historical data (Zweng and Münchow, 2006). In the western portion of Fram Strait, moored measurements over the last decade show mean AW temperature fluctuations on the order of 0.5°C (Schauer and others, 2008) for the pathway feeding AW to the northeast Greenland margins. Finally, the interannual variability in temperature in the deep waters in Nares Strait over the period 2003–09 is on the order of 0.1°C (Münchow and others, 2011). These values suggest that the variability of AW temperature in the fjords is largest for those at the margins of the Subpolar Gyre and of Baffin Bay, progressively less for those at the Nordic Seas' margins and smallest for those fjords connected to the Arctic Ocean. It is unclear whether the 1°C AW temperature difference in the winter/summer profiles at HG (Table 1) is due to interannual or seasonal variability. Thus, if AW temperature fluctuations are a major driver of glacier variability, then it is perhaps not surprising that the bulk of the glaciers that recently retreated are located at the margins of the Subpolar Gyre and Baffin Bay (Howat and others, 2007).

SUMMARY AND DISCUSSION

This study is the first attempt to compare and synthesize the characteristics of the ocean waters that melt the underside of Greenland's large glaciers, a process identified as a potential trigger of ice-sheet mass loss. By comparing ocean data recently collected from six of Greenland's glacier/fjord systems, spread across Greenland's three oceanic sectors, this study provides some insight into the mechanisms of glacier/ocean interaction and the variability of the oceanic forcing around Greenland. Of the glacier/fjord systems addressed here, three (Jakobshavn Isbræ and Helheim and Kangerdlugssuaq Glaciers) are part of the suite of glaciers that underwent rapid change in the later 1990s and early 2000s (Howat and others, 2007), and a fourth, Petermann Glacier, has recently lost a large portion of its floating ice tongue (Falkner and others, 2011). The other glaciers are presently stable.

Warm Atlantic Water from the subtropical North Atlantic Ocean is found at depth in all fjords, including near the glaciers, though its properties vary. The warmest waters are found near Helheim Glacier, Jakobshavn Isbræ, and Sermeq Kujalleq and Akangnardeq, while the coldest waters are found at Petermann Glacier. These differences reflect the routes taken by the AW to reach the three ocean basins around Greenland: the Subpolar Gyre and Baffin Bay, the Nordic Seas and the Arctic Ocean. The AW in the fjords is colder than that circulating offshore, indicating that these waters are transformed across the shelf. Though the fjord data are insufficient to map the interannual variation in properties, a review of the AW variability from the region outside the fjords suggests that the amplitude of the

interannual/decadal temperature variations also scales with distance from the source.

A comparison of the water properties in the fjords reveals some general characteristics. In all fjords the deep layer of AW is found below a cold layer of water of Arctic origin (Polar Water). Near the glaciers and during the summer, when the majority of the surveys were conducted, water properties indicate melting by AW and the release of subglacial discharge (runoff) at depth. In the two available winter surveys, we still find that AW drives melting but there is no subglacial discharge. These results indicate that the circulation at the ice edge is complex and influenced by the release of subglacial discharge at depth as well as by the fjord's stratification. They are consistent with recent theoretical and modeling studies indicating that subglacial discharge can strongly influence the plume dynamics at the ice edge (and the melt rate). The analysis presented is based on a number of limited surveys, but the general validity of the conclusions is supported by other existing data for many of these systems.

The results presented here have several important implications. They confirm that changes in the North Atlantic Ocean will be transmitted to Greenland's margins through the circulation of AW and that the timing and amplitude of any propagating anomaly will be different for each ocean basin. Indeed, distinct sectors of Greenland may experience opposite forcing due to oceanic variability since, for example, the Subpolar Gyre and the Nordic Seas tend to be out of phase in response to the North Atlantic Oscillation, the dominant mode of variability over the North Atlantic Ocean (Dickson and others, 1996). Since AW is likely modified by mixing with PW as it crosses the Greenland shelves and flows into the fjords, we speculate that changes at the glaciers' margins can also be driven by changes in PW (as argued by Andresen and others, 2012, for Helheim Glacier).

The results presented also highlight our limited knowledge of glacier/ocean interaction. The data painstakingly collected so far from the challenging environment of Greenland glacial fjords have been invaluable in shaping our initial understanding, but more data including repeat surveys, continuous time series and data from the upwelling region are crucially needed to improve our knowledge of these processes and our ability to model them.

ACKNOWLEDGEMENTS

F.S., D.A.S. and G.S.H. thank Melanie Duchin and Iris Menn, Captain P. Willcox and the crew of the *MV Arctic Sunrise*, Greenpeace International, J. Ryder and J. Kemp for their support in making the measurements near HG, KG and 79NG in summer 2009. F.S. and D.A.S acknowledge support from WHOI's Ocean and Climate Change Institute's Arctic Research Initiative and from US National Science Foundation grant NSF ARC-0909373. G.S.H., E.R. and Y.X. acknowledge support from NASA's Cryospheric Sciences Program. D.H. and C.G. acknowledge support from NSF ARC-0806393 and NASA NNX08AN52G. H.L.J acknowledges K. Falkner, A. Münchow and H. Melling, as well as support from the Canadian Federal Program for the International Polar Year, Fisheries and Oceans Canada, the US National Science Foundation and the Royal Society. She is also grateful to the captain, scientists and crew aboard the USCGC *Healy* and the CCGS *Henry Larsen*. K. Steffen kindly provided the PG data through the ice tongue.

REFERENCES

- Andersen ML and 14 others (2010) Spatial and temporal melt variability at Helheim Glacier, East Greenland, and its effect on ice dynamics. *J. Geophys. Res.*, **115**(F4), F04041 (doi: 10.1029/2010JF001760)
- Andresen CS and 10 others (2012) Rapid response of Helheim Glacier in Greenland to climate variability over the past century. *Nature Geosci.*, **5**(1), 37–41 (doi: 10.1038/ngeo1349)
- Azetsu-Scott K and Tan FC (1997) Oxygen isotope studies from Iceland to an East Greenland Fjord: behaviour of glacial meltwater plume. *Mar. Chem.*, **56**(3–4), 239–251 (doi: 10.1016/S0304-4203(96)00078-3)
- Bersch M, Yashayaev I and Koltermann KP (2007) Recent changes of the thermohaline circulation in the subpolar North Atlantic. *Ocean Dyn.*, **57**(3), 223–235 (doi: 10.1007/s10236-007-0104-7)
- Bower AS and 8 others (2002) Directly measured mid-depth circulation in the northeastern North Atlantic Ocean. *Nature*, **419**(6907), 603–607 (doi: 10.1038/nature01078)
- Budéus G, Schneider W and Kattner G (1997) Distribution and exchange of water masses in the Northeast Water Polynya (Greenland Sea). *J. Mar. Syst.*, **10**(1–4), 123–138 (doi: 10.1016/S0924-7963(96)00074-7)
- Christoffersen P and 7 others (2011) Warming of waters in an East Greenland fjord prior to glacier retreat: mechanisms and connection to large-scale atmospheric conditions. *Cryosphere*, **5**(3), 701–714 (doi: 10.5194/tc-5-701-2011)
- Cuny J, Rhines PB, Schott F and Lazier J (2005) Convection above the Labrador continental slope. *J. Phys. Oceanogr.*, **35**(4), 489–511 (doi: 10.1175/JPO2700.1)
- Curry B, Lee CM and Petrie B (2011) Volume, freshwater, and heat fluxes through Davis Strait, 2004–05. *J. Phys. Oceanogr.*, **41**(3), 429–436 (doi: 10.1175/2010JPO4536.1)
- De Steur L, Hansen E, Gerdes R, Karcher M, Fahrbach E and Holfort J (2009) Freshwater fluxes in the East Greenland Current: a decade of observations. *Geophys. Res. Lett.*, **36**(23), L23611 (doi: 10.1029/2009GL041278)
- Dickson R, Lazier J, Meincke J, Rhines P and Swift J (1996) Long-term coordinated changes in the convective activity of the North Atlantic. *Progr. Oceanogr.*, **38**(3), 241–295 (doi: 10.1016/S0079-6611(97)00002-5)
- Falkner KK and 11 others (2011) Context for the recent massive Petermann Glacier calving event. *Eos*, **92**(14), 117 (doi: 10.1029/2011EO140001)
- Fratantoni DM (2001) North Atlantic surface circulation during the 1990s observed with satellite-tracked drifters. *J. Geophys. Res.*, **106**(C10), 22 067–22 093 (doi: 10.1029/2000JC000730)
- Gade HG (1979) Melting of ice in sea water: a primitive model with application to the Antarctic ice shelf and icebergs. *J. Phys. Oceanogr.*, **9**(1), 189–198
- Hansen B and Østerhus S (2000) North Atlantic–Nordic Seas exchanges. *Progr. Oceanogr.*, **45**(2), 109–208 (doi: 10.1016/S0079-6611(99)00052-X)
- Holland DM, Thomas RH, de Young B, Ribergaard MH and Lyberth B (2008) Acceleration of Jakobshavn Isbrae triggered by warm subsurface ocean waters. *Nature Geosci.*, **1**(10), 659–664 (doi: 10.1038/ngeo316)
- Howat IM, Joughin IR and Scambos TA (2007) Rapid changes in ice discharge from Greenland outlet glaciers. *Science*, **315**(5818), 1559–1561 (doi: 10.1126/science.1138478)
- Huppert HE and Josberger EG (1980) The melting of ice in cold stratified water. *J. Phys. Oceanogr.*, **10**(6), 953–960
- Huppert HE and Turner JS (1980) Ice blocks melting into a salinity gradient. *J. Fluid Mech.*, **100**(2), 367–384 (doi: 10.1017/S0022112080001206)
- Isachsen PE, Mauritzen C and Svendsen H (2007) Dense water formation in the Nordic Seas diagnosed from sea surface buoyancy fluxes. *Deep-Sea Res. I*, **54**(1), 22–41 (doi: 10.1016/j.dsr.2006.09.008)
- Jakobsen PK, Ribergaard MH, Quadfasel D, Schmitt T and Hughes CW (2003) Near-surface circulation in the northern North

- Atlantic as inferred from Lagrangian drifters: variability from the mesoscale to interannual. *J. Geophys. Res.*, **108**(C8), 3251 (doi: 10.1029/2002JC001554)
- Jenkins A (1999) The impact of melting ice on ocean waters. *J. Phys. Oceanogr.*, **29**(9), 2370–2381
- Jenkins A (2011) Convection-driven melting near the grounding lines of ice shelves and tidewater glaciers. *J. Phys. Oceanogr.*, **41**(12), 2279–2294 (doi: 10.1175/JPO-D-11-03.1)
- Johnson HL, Münchow A, Falkner KK and Melling H (2011) Ocean circulation and properties in Petermann Fjord, Greenland. *J. Geophys. Res.*, **116**(C1), C01003 (doi: 10.1029/2010JC006519)
- Lloyd J and 6 others (2011) A 100 yr record of ocean temperature control on the stability of Jakobshavn Isbræ, West Greenland. *Geology*, **39**(9), 867–870 (doi: 10.1130/G32076.1)
- Mayer C, Reeh N, Jung-Rothenhäusler F, Huybrechts P and Oerter H (2000) The subglacial cavity and implied dynamics under Nioghalvfjerdsfjorden glacier, NE Greenland. *Geophys. Res. Lett.*, **27**(15), 2289–2292 (doi: 10.1029/2000GL011514)
- McCartney MS and Talley LD (1984) Warm-to-cold water conversion in the northern North Atlantic Ocean. *J. Phys. Oceanogr.*, **14**(5), 922–935 (doi: 10.1175/1520-0485(1984)014<0922:WTCWCI>2.0.CO;2)
- Mernild SH and Hasholt B (2009) Observed runoff, jökulhlaups and suspended sediment load from the Greenland ice sheet at Kangerlussuaq, West Greenland, 2007 and 2008. *J. Glaciol.*, **55**(193), 855–858 (doi: 10.3189/002214309790152465)
- Mortensen J, Lennert K, Bendtsen J and Rysgaard S (2011) Heat sources for glacial melt in a sub-Arctic fjord (Godthåbsfjord) in contact with the Greenland Ice Sheet. *J. Geophys. Res.*, **116**(C1), C01013 (doi: 10.1029/2010JC00652)
- Motyka RJ, Hunter L, Echelmeyer KA and Connor C (2003) Submarine melting at the terminus of a temperate tidewater glacier, LeConte Glacier, Alaska, U.S.A. *Ann. Glaciol.*, **36**, 57–65 (doi: 10.3189/172756403781816374)
- Motyka RJ, Truffer M, Fahnestock M, Mortensen J, Rysgaard S and Howat I (2011) Submarine melting of the 1985 Jakobshavn Isbræ floating tongue and the triggering of the current retreat. *J. Geophys. Res.*, **116**(F1), F01007 (doi: 10.1029/2009JF001632)
- Münchow A, Melling H and Falkner KK (2006) An observational estimate of volume and freshwater flux leaving the Arctic Ocean through Nares Strait. *J. Phys. Oceanogr.*, **36**(11), 2025–2041 (doi: 10.1175/JPO2962.1)
- Münchow A, Falkner KK, Melling H, Rabe B and Johnson HL (2011) Ocean warming of Nares Strait bottom waters off northwest Greenland, 2003–2009. *Oceanography*, **24**(3), 114–123 (doi: 10.5670/oceanog.2011.62)
- Nick FM, Vieli A, Howat IM and Joughin I (2009) Large-scale changes in Greenland outlet glacier dynamics triggered at the terminus. *Nature Geosci.*, **2**(2), 110–114 (doi: 10.1038/ngeo394)
- Orvik KA and Niiler P (2002) Major pathways of Atlantic water in the northern North Atlantic and Nordic Seas toward Arctic. *Geophys. Res. Lett.*, **29**(19), 1896 (doi: 10.1029/2002GL015002)
- Pickart RS and Spall MA (2007) Impact of Labrador Sea convection on the North Atlantic meridional overturning circulation. *J. Phys. Oceanogr.*, **37**(9), 2207–2227 (doi: 10.1175/JPO3178.1)
- Pritchard HD, Arthern RJ, Vaughan DG and Edwards LA (2009) Extensive dynamic thinning on the margins of the Greenland and Antarctic ice sheets. *Nature*, **461**(7266), 971–975 (doi: 10.1038/nature08471)
- Rignot E and Kanagaratnam P (2006) Changes in the velocity structure of the Greenland Ice Sheet. *Science*, **311**(5673), 986–990 (doi: 10.1126/science.1121381)
- Rignot E and Steffen K (2008) Channelized bottom melting and stability of floating ice shelves. *Geophys. Res. Lett.*, **35**(2), L02503 (doi: 10.1029/2007GL031765)
- Rignot E, Koppes M and Velicogna I (2010) Rapid submarine melting of the calving faces of West Greenland glaciers. *Nature Geosci.*, **3**(3), 141–218 (doi: 10.1038/ngeo765)
- Schauer U, Beszczynska-Möller A, Walczowski W, Fahrbach E, Piechura J and Hansen E (2008) Variation of measured heat flow through the Fram Strait between 1997 and 2006. In Dickson RR, Meincke J and Rhines P eds. *Arctic–subarctic ocean fluxes: defining the role of the northern seas in climate*. Springer, Dordrecht, 65–85
- Schjøth F, Andresen CS, Straneo F, Murray T, Scharrer K and Koralev A (2012) Campaign to map the bathymetry of a major Greenland fjord. *Eos*, **93**(14), 141 (doi: 10.1029/2012EO14001)
- Schott FA and Brandt P (2007) Circulation and deep water export of the subpolar North Atlantic during the 1990s. In Schmittner A, Chiang J and Hemmings S eds. *Ocean circulation: mechanisms and impacts*. American Geophysical Union, Washington, DC, 91–118 (Geophysical Monograph Series 173)
- Schumann K, Völker D and Weinrebe WR (2012) Acoustic mapping of the Ilulissat Ice Fjord mouth, West Greenland. *Quat. Sci. Rev.*, **40**, 78–88
- Solomon S and 7 others eds. (2007) *Climate change 2007: the physical science basis. Contribution of Working Group I to the Fourth Assessment Report of the Intergovernmental Panel on Climate Change*. Cambridge University Press, Cambridge
- Straneo F and 7 others (2010) Rapid circulation of warm subtropical waters in a major glacial fjord in East Greenland. *Nature Geosci.*, **3**(33), 182–186 (doi: 10.1038/ngeo764)
- Straneo F and 6 others (2011) Impact of fjord dynamics and glacial runoff on the circulation near Helheim Glacier. *Nature Geosci.*, **4**(5), 322–327 (doi: 10.1038/ngeo1109)
- Sutherland DA and Pickart RS (2008) The East Greenland Coastal Current: structure, variability, and forcing. *Progr. Oceanogr.*, **78**(1), 58–77 (doi: 10.1016/j.pocean.2007.09.006)
- Sutherland D and Straneo F (2012) Estimating ocean heat transports and submarine melt rates in Sermilik Fjord, Greenland, using lowered ADCP velocity profiles. *Ann. Glaciol.*, **53**(60 Pt 1), 50–58
- Thierry V, de Boisséson E and Mercier H (2008) Interannual variability of the Subpolar Mode Water properties over the Reykjanes Ridge during 1990–2006. *J. Geophys. Res.*, **113**(C4), C04016 (doi: 10.1029/2007JC004443)
- Thomas RH (2004) Force-perturbation analysis of recent thinning and acceleration of Jakobshavn Isbræ, Greenland. *J. Glaciol.*, **50**(168), 57–66 (doi: 10.3189/172756504781830321)
- Våge K and 9 others (2011) The Irminger Gyre: circulation, convection, and interannual variability. *Deep-Sea Res. I*, **58**(5), 590–614 (doi: 10.1016/j.dsr.2011.03.001)
- Van den Broeke M and 8 others (2009) Partitioning recent Greenland mass loss. *Science*, **326**(5955), 984–986 (doi: 10.1126/science.1178176)
- Vieli A and Nick FM (2011) Understanding and modelling rapid dynamic changes of tidewater outlet glaciers: issues and implications. *Surv. Geophys.*, **32**(4–5), 437–458 (doi: 10.1007/s10712-011-9132-4)
- Xu Y, Rignot E, Menemenlis D and Koppes MN (2012) Numerical experiments on subaqueous melting of Greenland tidewater glaciers in response to ocean warming and enhanced subglacial runoff. *Ann. Glaciol.*, **53**(60 Pt 2) (see paper in this issue)
- Zweng MM and Münchow A (2006) Warming and freshening of Baffin Bay, 1916–2003. *J. Geophys. Res.*, **111**(C7), C07016 (doi: 10.1029/2005JC003093)